Advanced Battery Materials Research at Nazarbayev University: Review

I. Kurmanbayeva[1], A. Mentbayeva[2], A. Nurpeissova[1], Z. Bakenov[1,2]*

[1]National Laboratory Astana, 53 Kabanbay batyr ave., Nur-Sultan, Kazakhstan
[2]School of Engineering, Nazarbayev University, 53 Kabanbay batyr ave., Nur-Sultan, Kazakhstan

Article info

Abstract

With the rapid development of new and advanced technologies, the request for energy storage device with better electrochemical characteristics is increasing as well. Therefore, the search and development for more novel and efficient energy storage components are imperative. In Kazakhstan there are several groups that were established to conduct research in the field of energy storage devices. One of them is professor Mansurov's research group with we have a long time fruitful collaboration. Group at Nazarbayev University do research in design and investigation of advanced energy storage materials for high performance energy storage devices, including lithium-ion batteries, sodium-ion batteries, lithium-sulfur batteries, and aqueous rechargeable batteries, employing strategies as nanostructuring, nano/micro combination, hybridization, pore-structure control, configuration design, 3D printing, surface modification, and composition optimization. This manuscript reviews research on advanced battery materials, provided by Nazarbayev University scientists since the last 10 years.

1. Multifunctional materials for Li-S batteries

Sulfur being inexpensive, abundant and ecologically friendly, has attractive advantages such as high theoretical specific capacity (1675 mAh g^{-1}) and energy density (2600 Wh kg^{-1}) [1]. Therefore, Li-S batteries are considered as promising energy storage systems in post Li-ion batteries. Despite the attractive advantages of sulfur, commercialization of Li-S batteries is hindered due to several problems of sulfur associated with low electrical conductivity of sulfur, complicated redox reactions (formation of intermediate products lithium polysulfides (LiPSs), which dissolve in liquid electrolyte and migrate back and forward to anode side, the "shuttle effect" phenomenon) and significant volume changes upon reduction of sulfur to lithium sulfides [2]. In order to solve above mentioned problems various strategies were developed. On the most attractive way is the implementation of porous carbon additives to sulfur, which is designed to increase the conductivity and buffer volume changes of sulfur and lithium sulfide. However,

low intermolecular forces between non-polar carbon and polar LiPSs are incapable of fully preventing shuttle effect. Therefore, in recent years hybrid materials (metal compounds with porous carbon) gained serious attention due to the polar nature of metal compounds which can effectively catch polar LiPSs. Moreover, transition metal compounds used in other electrochemical reactions as electrocatalysts can facilitate the conversion of LiPSs to lithium sulfides and vice versa. In this way, the role of metal oxides such as $Mg_{0.6}Ni_{0.4}O$ [1, 3, 4], ZnO [5, 6], Fe/Co_3O_4 [7] Co_3O_{4-x} [8], Fe_3O_4 [9], TiO_2 [10] and TiO_{2-x} [11] as sulfur and LiPSs carriers and the role of Ni [12, 13], Co [14] and Fe [7] electrocatalysts and hetero-structured materials were investigated.

The earliest works on the use of metal oxides started with the nickel manganese oxide ($Mg_{0.6}Ni_{0.4}O$) particles which were used as sulfur carriers to prepare $S/Mg_{0.6}Ni_{0.4}O$ and additives to sulfur polyacrylonitrile (S/PAN) composites. $Mg_{0.6}Ni_{0.4}O$ particles used as a sulfur host resulted in poor performance of Li-S batteries due to the low electrical conductivity. Among other 3d transition metals, titanium, cobalt and iron oxides

*Corresponding author. E-mail: zbakenov@nu.edu.kz

Table 1
Metal oxide compounds used in Li-S batteries

Metal oxide compound	Role	Method of synthesis	Sulfur loading, mg cm^{-2}	Reversible capacity, mAhg^{-1}	Ref.
$Mg_{0.6}Ni_{0.4}O$	Sulfur host	SHS	-	850 at 0.1C	[1]
$Mg_{0.6}Ni_{0.4}O/PAN$	Additive	SHS	-	1223 at 0.1C	[3]
$Mg_{0.6}Ni_{0.4}O/PANi$	Additive	SHS	-	1448 at 0.1C	[4]
3DOMPPy@ZnO	Immobilizers	Template assisted	Up to 5	794.5 after 300 cycles	[5]
ZnO@NCNT	Immobilizers	Sol-gel	Up to 4.75	1032 at 0.2C	[6]
Fe/Co_3O_4	Sulfur carrier	Hydrothermal	-	571.3 at 5C	[7]
Co_3O_{4-x}	Sulfur host	Hydrothermal	2	1256 at 0.2C	[8]
$Fe_3O_4@C-Gr$	Sulfur host	Hydrothermal	2	1425 at 0.2C	[9]
$3DOM-mTiO_2$	Sulfur host	Template assisted	-	1089 at 0.2C	[10]
TiO_{2-x}/rGO	Sulfur host	Hydrothermal	1.5	700 at 1.0C	[11]

$(TiO_{2-x}/rGO, Co_3O_{4-x}, Fe_3O_4@C-Gr)$ used as a sulfur carriers and hosts showed extremely high electrochemical performance, which can be explained by the strong energy binding between polar LiPSs and metal oxides (Table 1). The major advantage of using these compounds is related with the ease of synthesis such as hydrothermal method, which can yield uniform spherical, microparticles for uniform distribution of sulfur and sulfur intermediate products.

Despite the strong interaction of metal oxides with polar LiPSs, limited number of polar active sites and large particle size the electrochemical performance of Li-S batteries is limited. This can be attributed to the low kinetics of sulfur conversion to lithium sulfides and vice versa. Therefore, in order to facilitate the conversion of sulfur to end products, effective catalysts need to be designed. Among metal catalysts 3d transition metals such Ni, Co and Fe are considered as promising catalysts compared with noble metals due to low cost of precursors and high abundance. Since metals have poor interaction with polar LiPSs, in order to limit the shuttle effect, sulfur active material needs to be injected into pores of porous carbon or polar hosts such as metal oxide or phosphide. Generally using porous nickel phosphide and cobalt oxide sulfur hosts with Fe and Ni electrocatalysts (Fe/Co_3O_4 and Ni/$Ni_2P@C$) delivered high reversible capacity at high current densities (571.3 mAh g^{-1} at 5C and 716.9 mAh g^{-1} at 3C, respectively) [12, 13]. Such high reversible capacity at high current density can be attributed to the strong binding between metal oxides and LiPSs and catalytic activity of Fe and Ni electrocatalysts. Increasing the number of electrocatalytic sites further enhanced the electrochemical performance of Li-S batteries when the cobalt nickel porous carbon nanofiber (CoNi@PCNF) was used as a 3D current collector (Fig. 1) [12]. Moreover, CoNi@PCNF was further used as current collector for lithium, which allowed assembling Li-S full cell, with extremely high electrochemical performance (about 785 mAh g^{-1}).
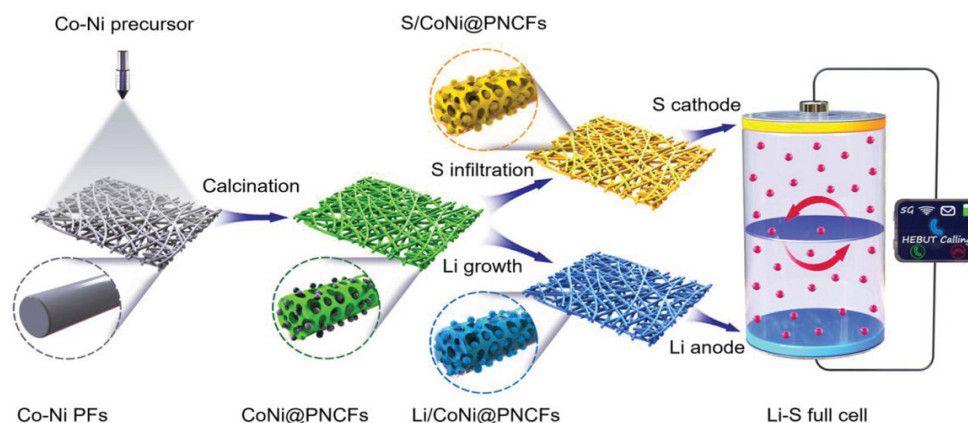

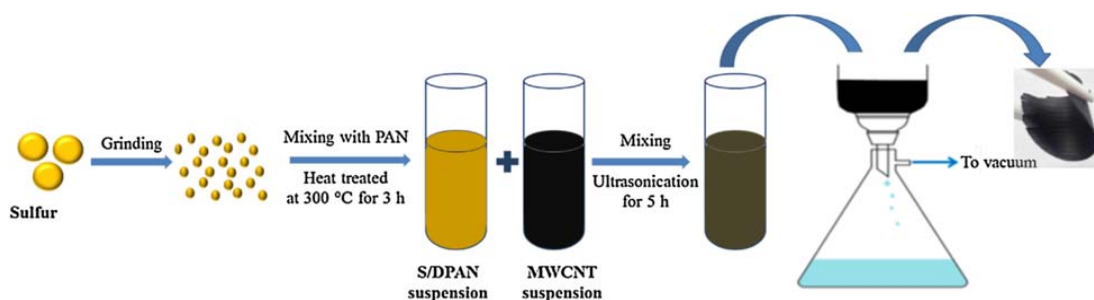
Fig. 1. CoNi@PCNF all-purpose electrode design [12].

Fig. 2. Schematics of preparation of freestanding S/DPAN/MWCNT composite cathode [15].

The high electrochemical performance of Li-S full cell can be explained with effective encapsulation of sulfur and high conductivity of carbon nanofibers. Also, the addition of conductive additives and a binder leads to a significant decrease in the total gravimetric capacity of the sulfur cathode. Thus, eliminating the binder and current collector by forming a free-standing electrode can simplify its manufacturing and significantly increase the energy density of the batteries due to reduction in content of the electrochemically active component. Therefore, it has been proposed to prepare a sulfur-based cathode without the use of heavy metal current collectors and inactive polymer binders, such as the penetration of sulfur into activated carbon fiber or paper like. As reported by Mentbayeva et al., a freestanding cathode composite of sulfur/dehydrogenated polyacrylonitrile/multiwalled carbon nanotube (S/DPAN/MWCNT) was prepared by a simple vacuum filtration method (Fig. 2). This design effectively exploits the synergistic effect of the ability of the conductive pyrolyzed polyacrylonitrile matrix to covalently bind sulfur, ensuring its uniform distribution, and the high conductivity of the MWCNT network with excellent mechanical stability [15]. Zhao et al. first introduced a carbon nanotube composite (S/N-CNT), which does not contain a binder and doped with sulfur/nitrogen (S/N-CNT), obtained by simple mixing of solutions, as a cathode material for Li/S batteries. It has been demonstrated that the use of N-CNTs has resulted in high electrochemical performance, indicating the great potential of N-CNTs as a cathode additive for high-performance lithium-sulfur batteries [16].

In addition, one of the key characteristics of electronic devices is their flexibility due to the growing demand for such technologies. Thus, Kalybekkyzy and other authors fabricated a flexible nanofiber composite by simple electrospinning technique and tested it as a freestanding cathode for high-performance flexible lithium/sulfur bat-
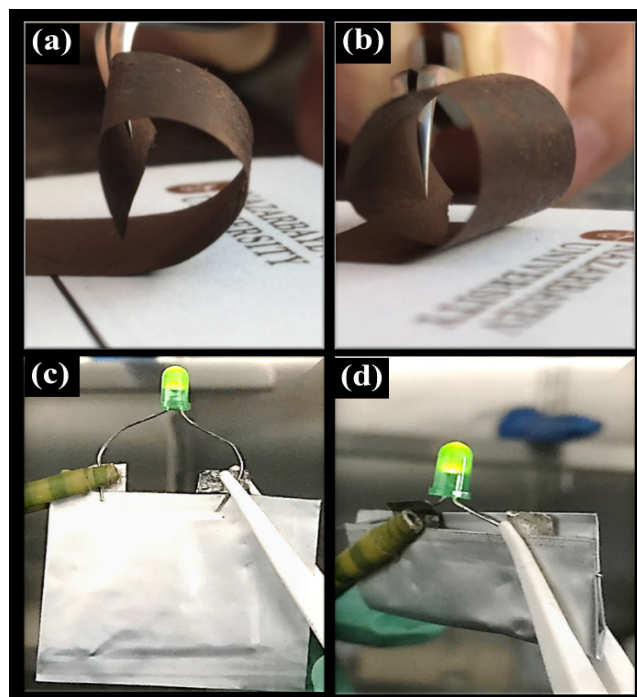

Fig. 3. Images demonstrating (a, b) the freestanding flexible nanofiber composite cathode and (c) illustration of pouch cell with nanofiber composite cathode powering LED lamps under normal static condition and (d) under being manually bent [17].

teries (Fig. 3). Due to its structural features, the prepared nanofiber cathode had good compatibility with conventional carbonates-based electrolytes and showed high coulombic efficiency, long service life [17].

Due to the three-dimensional (3D) structure, carbon fiber fabric has attracted great interest as a substrate and/or current collector, which has the ability to incorporate various materials into its 3D structure, providing higher interfacial interaction compared to 2D collectors. The use of a carbon fiber current collector in a lithium-sulfur battery allows for a high sulfur content in its three-dimensional geometric structure, which provides increased electronic conductivity between high-conductivity

carbon particles and low-conductivity sulfur particles. With this purpose, Zhang et al. fabricated carbon fiber fabric and nickel foam as current collectors for a composite sulfur cathode in the structure of a lithium cell. It has been suggested that the advantages of carbon fiber over Ni foam are due to its inherent chemical, structural and morphological uniqueness, which, along with its known high conductivity and chemical inertia, provides increased affinity for the sulfur composite cathode and improves stable charge transfer conditions during battery operation [18]. Similar work was done by Kalybekkyzy et al., where a lightweight carbon nanofibers (CNFs) fabricated by a simple electrospinning method and used as a 3D structured current collector for a sulfur cathode which ensure the compact packing of active material and provide high bulk conductivity of the electrode. The light wight of CNF current collector and high sulfur areal mass loading resulted in improved capacity for the whole mass of mAh g^{-1}, while the conventional one on Al foil offered 200 mAh g^{-1}. Therefore, the capacity of the electrode was increased 2.5 times by replacing the Al foil with an ultralight and porous cPAN CNF current collector [19].

Another work carried out by Qui et al. is aimed at developing an improved composite obtained from an organometallic titanium framework as a substrate for the placement of sulfur as illustrated in Fig. 4. The manufactured TiO_2 porous matrix provides sufficient pore volume to store the sulfur and buffer its volumetric expansion during the charge/discharge process. In addition, Co_3O_4 nanoparticles with strong polarity activate enhanced interactions with polysulfides and have different adsorption and electrocatalytic sites that can contribute to the intermediate LiPS conversion reaction. Furthermore, a carbon nanotube improves the contact between S/Li_2S and the host material and strengthen the structural integrity and stability of the composite cathode [20].

Along with the advancement of sulfur composite cathode and conductive host materials, the development of gel and solid polymer electrolytes is promising way to overcome the issues of Li-S batteries. Bakenov's group prepared gel polymer electrolyte (GPE) based on poly(vinylidene fluoride-co-hexafluoropropylene)/poly(methylmethacrylate)/ nanoclay (PVDF-HFP/PMMA/MMT) composite matrix by phase separation method [21]. The mechanically stable, porous membranes were activated lithium hexafluorophosphate solution. The performance of the material as an electrolyte for Li/S battery was evaluated in cells containing a ternary sulfur/polyacrylonitrile/$Mg_{0.6}Ni_{0.4}O$ (S/PAN/$Mg_{0.6}Ni_{0.4}O$) composite cathode which was developed previously [3]. According to the results, GPE is electrochemically stable in the 1 to 3.5 V vs. Li^+/Li range, ionic conductivity is equal to 3.06 mS cm^{-1} at room temperature, Li|PVDF-HFP/PMMA/MMT GPE|S/PAN/ $Mg_{0.6}Ni_{0.4}O$ cell shows a high coulombic efficiency (above 99%) over 100 cycles, discharge capacity after 100 cycles at 0.1 C is 1.071 mAh g^{-1}.

Another GPE was prepared by trapping a liquid electrolyte in a PVDF-HFP/PMMA polymer matrix doped with silicon dioxide (SiO_2) nanoparticles [22]. The GPE exhibited a highly porous structure, which provided a high surface area to the membrane and enhances its absorption ability and as a result GPE had high electrolyte uptake (71%). The GPE membrane is electrochemically stable in the operation range of Li|S cell between 1 and 3 V vs. Li^+/Li and shows a high ionic conductivity of 3.12 mS cm^{-1} at room temperature. Li|GPE|S cell with the S/GNS composite cathode delivers a high initial discharge capacity of about 809 mAh g^{-1} at 0.2C rate and exhibits an enhanced cyclability. A combination of the S/GNS composite cathode and PVDF-HFP/ PMMA/SiO_2 GPE plays a significant role in retarding a shuttle effect.
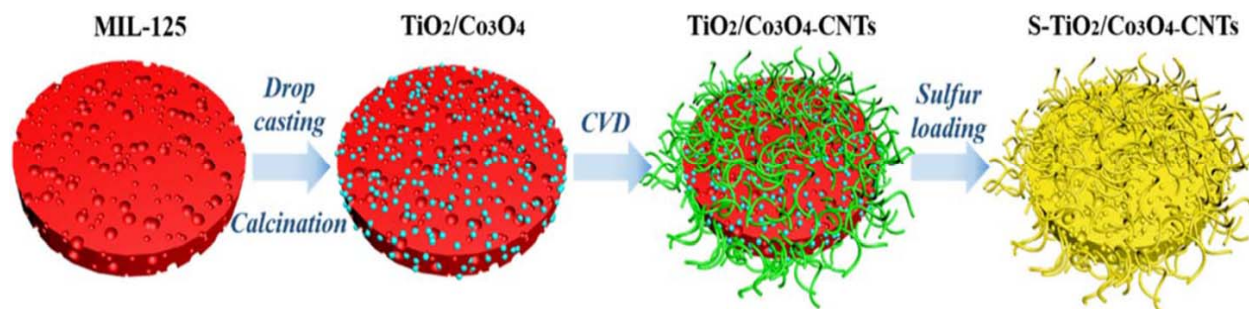

Fig. 4. Schematics of S–TiO_2/Co_3O_4-CNTs composite preparation [20].

Alternatively, there are works on improvement of Li-S battery performance by surface modification of polypropylene separator. Ultrathin, lightweight clay-containing layer-by-layer coating [23] and a novel hierarchically porous polypyrrole sphere (PPS) modified separator [24] were developed. The modified separator was prepared by coating of commercial polypropylene (PP) separator with polyethylene imine (PEI), clay nanoparticles and poly(acrylic acid) (PAA) by layer-by-layer technique. The coated separator showed better mechanical, thermal properties, electrolyte uptake compared with bare separator. The coating inhibited polysulfide diffusion and improved electrochemical performance of the Li-S cell, the Coulombic efficiency was increased from 50 to 99%). In another work the hierarchically porous PPS modified separator was prepared by casting PPS composite to the PP separator. According to the polysulfide penetration test, the PPS modified separator could effectively suppress shutting effect. The EIS measurements showed that the cell with the PPS-modified separator has a smaller charge transfer resistance than with the routine separator, which can be due to the excellent conductivity of the PPS coating layer. The cell with the PPS-modified separator delivered the discharge capacity of 855 mAh g^{-1} and retained a high efficiency of more than 94% over 100 cycles at 0.2 C (the cell with the routine separator only delivered 559 mAh g^{-1} over 100 cycles).

Summarizing, a comprehensive consideration of all cell components, including comprising effect of the components operation/performance on each other, should be taken as a global goal, and only in this case there could be a complex and remarkable step towards creating a stable and safe long-operating Li-S battery. By virtue of the previous strategies that have been provided by the researches and concentration of the efforts to overcome the obstacles upon the commercialization process, it is hopeful that practical Li-S batteries are coming in the foreseeable future.

2. Current state of 3D structured energy storage devices

Recently a rapid technological progress in various fields of industry and daily life has been driven by miniaturization of electronics. Components such as hearing aids, spy cameras, heart monitors, implantable orthodontic systems, logic and memory circuits with various sensors, and military cyborg drones, etc. have been drastically reduced to smaller dimensions with vastly improved performance (Fig. 5). Limited performance of batteries is one of the most critical problems to be tackled for sustainable technological advances and to allow for further development of novel and future technologies.

Lithium-ion batteries (LIBs) exhibit excellent cycle performance and high energy capacity and thus are the best choice to power miniaturized devices. However, the current architecture used in LIBs' electrodes limits the energy and power densities in electrodes. Furthermore, safety issues arising from flammable liquid electrolytes and lithium dendrite growth upon cycling still remain as the major challenges for implementation of LIBs in this area. Advanced architectures and materials are needed to design high performance LIBs with increased energy storage capacity per unit volume

Fig. 5. Present and novel future technologies with integrated LIBs.

while maintaining a small footprint area. Recently, 3D solid-state batteries with enhanced energy and power densities are receiving great attention due to their intrinsic safety and great flexibility in device design and integration. Nonetheless, the fabrication of 3D solid-state batteries has been a formidable challenge due to the limitation of conventional thin-film techniques [25]. However, despite difficulties, several 3D solid-state battery concepts were realized and investigated. Peter H.L. Notten et al. proposed a concept based on the step-conformal deposition of various (in)active layers on a high surface area silicon substrates obtained by micro-etching (Fig. 6a), while Nathan et al. used isotropic 3D configuration, seen in Fig. 6b, that can be fabricated by successive deposition of conformal films. Latter battery was one of the first 'functioning full 3D' lithium ion microbatteries [26].

Even though the 3D designs of battery concepts were proved to be realizable, there are still unanswered questions about the kinetics, interphase diffusion of Li^+-ions, integration and fabrication techniques that need our immediate attention. Therefore, our group focuses on the development of 3D electrodes, 3D current collectors and 3D all solid-state batteries fabricated by various methods with the consequent investigation of their electrochemical properties.
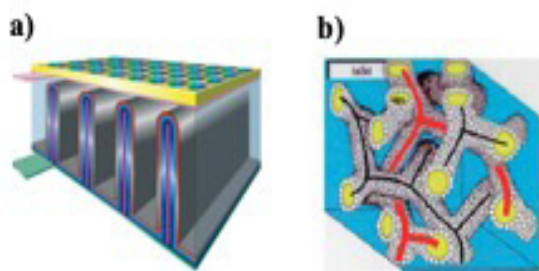

Fig. 6. 3D solid-state batteries: step-conformal deposited (a); isotropic 3D configuration (b) [25, 26].

Mainly 3D structured electrode architectures come in different forms such as interdigitated, honeycomb, porous three dimensional and interwoven structures as seen in Fig. 7.

Using foam structure allows obtaining a tremendous surface area, high mesoporosity, good electric conductivity, and an excellent chemical stability in a wide variety of liquid electrolytes. Nurpeissova et. al. reported a unique 3D architecture anode fabricated by electrodeposition of ultrathin Ni_3Sn_4 intermetallic alloy onto a commercially available nickel foam current collector from an aqueous electrolyte [28–31]. The designed three-dimensional electrode demonstrated a high discharge capacity of 843.75 mAh g^{-1} during initial cycles and an improved cycle performance over 100 cycles in contrast with the same alloy electrodeposited onto planar substrate (Fig. 8). The high surface area of the electrode and short L^+-ions diffusion paths along with suppression of volume expansion provided by the proposed 3D structure and Ni inactive matrix play a key role in improving the performance of the electrode.

Yet another work worth mentioning is the Si on the Ni foam. 3D structured composite anode containing silicon thin film on graphene coated Ni foam was prepared by chemical vapor deposition and magnetron sputtering techniques [32] by Mukanova et al. As the main problem of the Si is the huge volume expansion, the 3D structure of the current collector is capable of effectively suppress/diminish the volume changes, maintaining stable structure upon cycling. Along with this, graphene serves as an additional electrochemically active component and provides improved conductivity. Designed anode exhibits a high areal capacity of around 75 µAh cm^{-2} upon 500 cycles with the coulombic efficiency of around 99%.

Along with Ni foams, commercially available Cu foams were also utilized in many works to support the 3D architecture. In her work, Kalimuldina
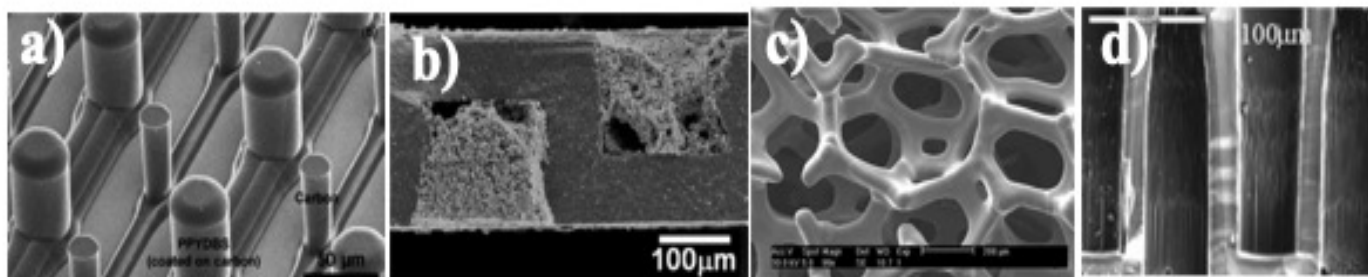

Fig. 7. 3D-electrode architectures: interdigitated structure (a); honeycomb structure (b); porous three-dimensional structure (c); interwoven structure (d) [27].
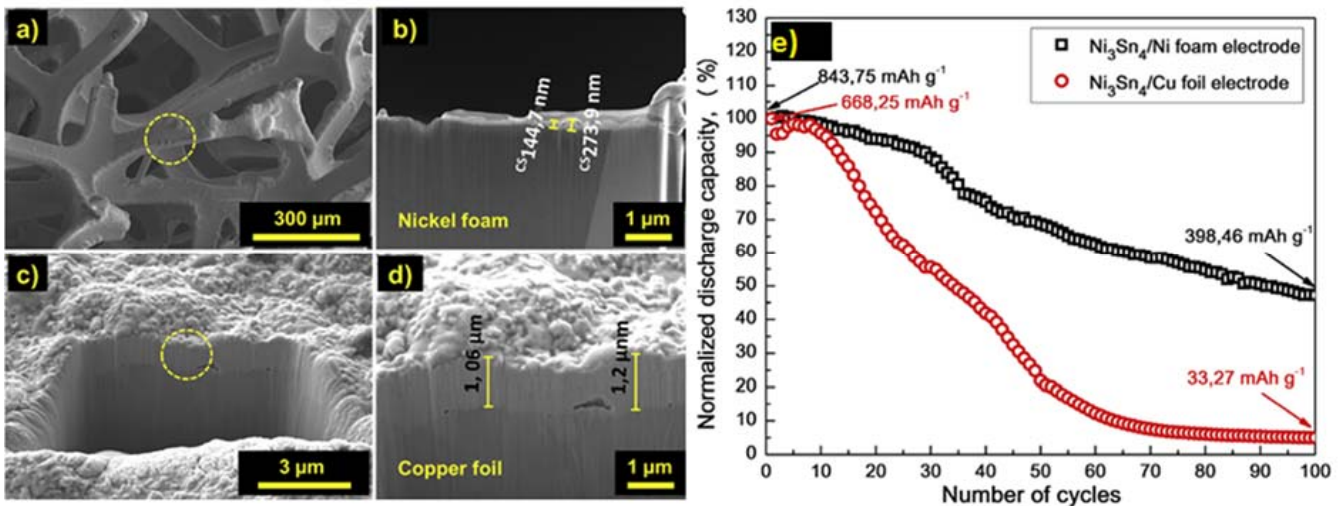
Fig. 8. SEM (a, c), TEM (b, d) images and electrochemical performance (e) of 2D and 3D Ni$_3$Sn$_4$ intermetallic alloys [31].

et al. fabricated conductive and flexible CuS with a unique hierarchical nanocrystalline branches and and Cu$_2$S nanoflower films directly grown on three-dimensional (3D) porous Cu foam using an easy and facile solution processing method without a binder and conductive agent for the first time. Copper sulfides (Cu$_x$S) with different stoichiometry are considered as prospective cathode materials for lithium batteries owing to their large energy storage capability [33]. The synthesis procedure is quick and does not require complex routes. Electrochemical testing of Cu$_x$S/Cu foam elec-

trodes (x=1, 1.8) showed a reasonable capacities of 450 mAh g^{-1} and 250 mAh g^{-1} at 0.1 C and excellent cyclability, which might be attributed to the unique 3D structure of the current collector and hierarchical nanocrystalline branches and nanoflowers that provide fast diffusion and a large surface area (Fig. 9) [34, 35].

Obtained results using Ni and Cu foams suggest that the better electrochemical performance of 3D electrodes is attributed to the unique structure of foams that effectively increased the contact area between electrolyte and electrode.
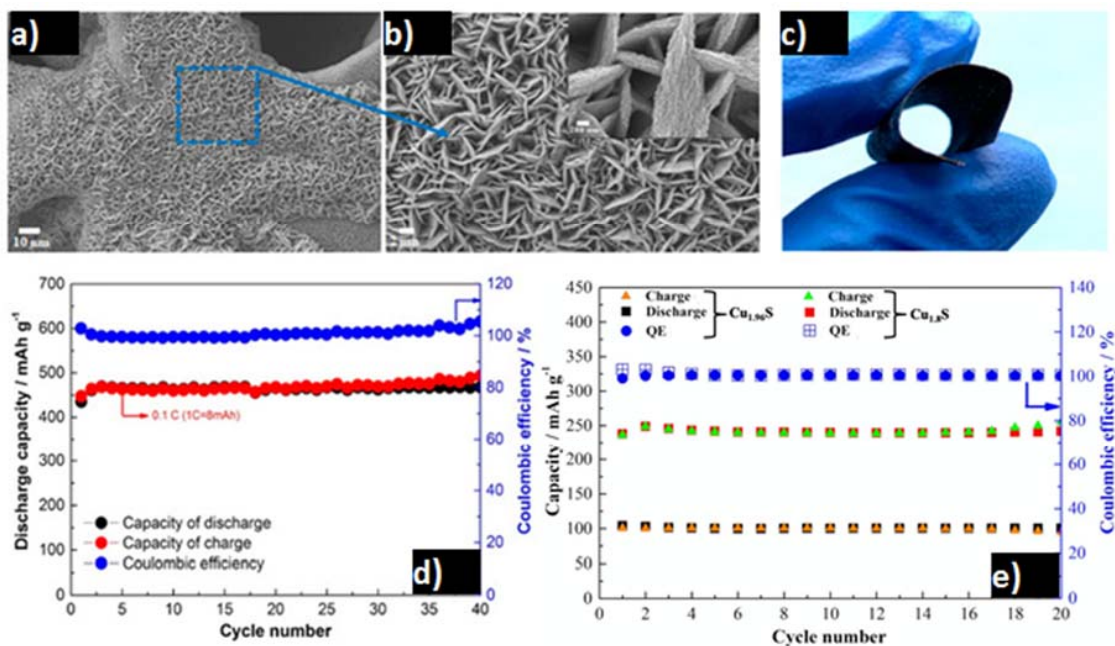

Fig. 9. SEM images (a,b) and photograph showing flexibility of 3D CuS/Cu films; electrochemical performance of 3D CuS/Cu films (d) and 3D Cu1.8S/Cu films (e) [34, 35].

In 2013 Prieto Battery published a patent for an innovative three-dimensional battery that radically differs from modern counterparts in its unique combination of components and architecture design. The patented technology is based on a porous copper structure (copper foam), which is located in an ultra-thin layer of polymer electrolyte wrapped in a cathode matrix. The result is a lithium-ion battery with a three-dimensional structure, consisting of interpenetrating electrodes with extremely close distances for ion diffusion processes. The power density of such batteries can reach 14.000 W/L, which is an order of magnitude higher than the indicators of the used two-dimensional structures [36]. Based on the above possibilities for improving battery performance, Mentbayeva et al. reported on the development of a full 3D battery composed of Ni_3Sn_4 (Ni–Sn) alloy electrodeposited onto a nickel foam current collector to form a 3D anode, which was coated with a polymer electrolyte-separator film, and $LiFePO_4$/CNT cathode filled into the voids of the resulting 3D structure, as depicted in Fig. 10 [37].

The prepared full 3D battery successfully operated at 0.1C rate and retained 90% of its initial capacity over 100 galvanostatic charge-discharge cycles [37].

Additive manufacturing, also known as 3D printing, has appeared as a novel class of free form fabrication technologies that have a variety of possibilities for the rapid creation of complex architectures at lower cost than conventional methods. 3D printing enables the controlled creation of functional materials with three-dimensional architectures, representing a promising approach for the fabrication of next-generation electrochemical energy-storage devices and has many unique advantages over conventional manufacturing methods. Moreover, sequential 3D printing of battery electrodes and the solid electrolyte layer meets the need for intimate contact between the electrodes and electrolytes. The exclusive capabilities of the 3D-printing technology enable the design of different shapes and high-surface-area structures, which no other manufacturing method can easily do. Therefore, the use of 3D printing will
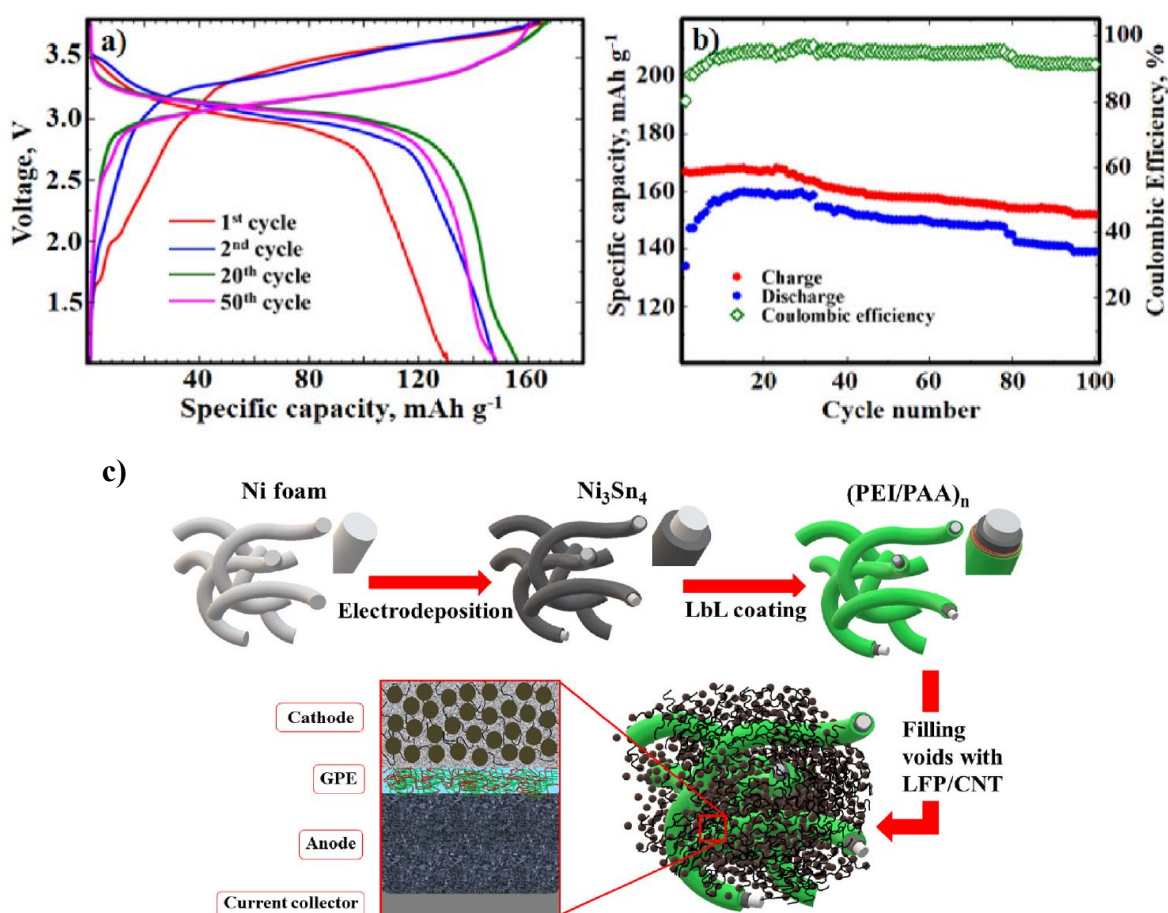

Fig. 10. Galvanostatic charge and discharge profile (a), cyclability and coulombic efficiency at 0.1C (b) and Schematic illustration of 3D full battery fabrication and configuration of 3D full battery (c) [37].

provide an ideal opportunity to design high-power micro batteries with well-designed arrangements of microelectrodes [38]. Electrodes in most of the printed batteries are prepared by extrusion-based methods. Extrusion-based 3D printing employs a three-axis motion stage to draw patterns by robotically squeezing "ink" through a micro-nozzle. Based on this concept, various 3D forms of micro batteries from simple to complex have been proposed and are currently being studied. The pioneer of 3D printed batteries, Dr. Lewis from Harvard was able to print a battery with a few micrometer dimensions with outstanding performance as seen in Fig. 11.

The 3D-printed $LiFePO_4/Li_4Ti_5O_{12}$ full cell features initial charge and discharge capacities of 117 and 91 mA h g^{-1} with good cycling stability. Highly concentrated inks were prepared by dispersing the particles in ethylene glycol (EG) – water solution [40, 15]. After her investigations, several groups also reported on the 3D printed batteries. For example, Hu et al. reported on the 3D structured battery by slurry extrusion from an air-powered dispenser, of a novel synthesized cathode comprising $LiMn_{0.21}Fe_{0.79}PO_4$-C nanocrystals [41]. Considering the novelty of this direction, our group will work on the direction of 3D printing.

3. Rechargeable aqueous lithium-ion battery (RALIB)

Even lithium-ion batteries are the leading energy source for portable devices, they are associated with safety concerns due to the use of organic flammable electrolytes. Another problem of LIB is their high price, where 45% of which is the cost of technological requirements (special conditions for assembling batteries due to the sensitivity of materials to air and moisture, the use of expensive packaging). Therefore, the attention of researchers in recent decades is directed to the development of such systems in which it is possible to combine the
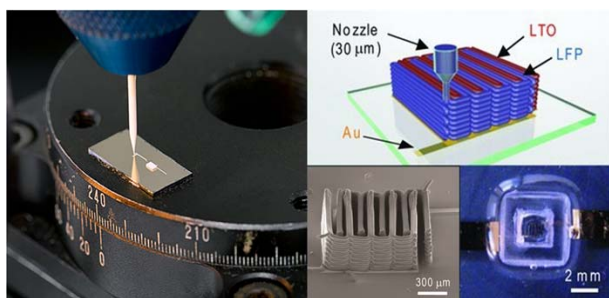

Fig. 11. 3D printed microbattery [39].

Table 2
Comparison of battery technology costs

	LIB	RALIB	Lead Acid Battery
Battery Cost (USD/KWh)	600	170	170
Working Voltage, V	3.0	1.2	2.0
Cycle life (#)	2000	1000	1000 (25 °C); 500 (33 °C)
Efficiency (η)	100	100	50-95
Energy Density (Wh/Kg)	100-150	40-60	30-40
Lifetime cost (USD/KWh)	0.30	0.17	0.23 (25 °C); 0.50 (33 °C)

stability and energy density of LIB with safety and reduced cost (Table 2).

Our group developed the model of zinc based Rechargeable Aqueous Lithium-ion Battery (RALIB) $Zn/LiCl-ZnCl_2/LiFePO_4$ with a mild acidic electrolyte [42, 43]. The concept is demonstrated using $LiFePO_4$ cathode and Zn anode, operating in an optimized weak acidic aqueous Li^+/Zn^{2+} binary electrolyte. Rechargeable aqueous lithium-ion battery technology is very attractive, especially for large scale applications, including transportation, because the ionic conductivity of aqueous electrolytes is greater than that of organic counterparts, thereby allowing higher electrochemical reaction rates, and negligible potential drops due to the electrolyte impedance. In contrast with non-aqueous lithium batteries (LIB), the operation voltages of batteries with aqueous electrolytes are restricted by the electrochemical stability of water. The water stability window is pH-dependent because the hydrogen evolution potential is pH-dependent. Zinc metal is considered as a promising anode material for rechargeable batteries due to its high theoretical capacity (820 mAh g^{-1}), abundance, safety, scalability, low cost and environmentally friendliness [44, 45]. However, zinc is thermodynamically unstable in the aqueous environment [46, 47]. It dissolves into Zn^{2+} ions under acidic conditions (pH<4), more stable at neutral pH, and it's solubility increases in alkaline media. Commercial, mainly used as primary batteries, aqueous zinc batteries (Zn-air, Zn-MnO$_2$ and etc.) have alkaline media [48], where $Zn(OH)_4^{-2}$ complexes formed due to the abundance of OH$^-$ ions. These zincate ions precipitate in the form of ZnO, resulting in dendrite growth or passivation of the anode.

Mildly acidic aqueous (or neutral) electrolyte for lithium-ion batteries is being investigated relatively recently [49]. Main electrochemical performance of the developed Zn/LiCl-ZnCl$_2$/LiFePO$_4$ system is presented in Fig. 12.

Rate capability performance (Fig. 12a) shows that the specific capacity gradually decreases with the current density increase. Notwithstanding, the capacity is fully recovered when the cycling rate is switched back to 0.6 C, indicating that along with superior rate capability, the Zn/LiClZnCl$_2$/LiFePO$_4$ battery system possesses a very high reversibility and electrochemical stability [42]. The LiFePO$_4$ positive electrode exhibited 400 cycles with 85% capacity retention and 100% energy efficiency at 6 C rate (Fig. 12b). It means that the battery is fully charged and discharged in 10 min. The novel battery temperature tolerance is also promising. It shows high capacity retention at various temperatures ranging from -10 to 50 °C. The system provides an operating voltage of 1.2 V. The electrochemical mechanism of the Zn/LiFePO$_4$ battery operation is illustrated in Fig. 12c. During the charge process, at the positive electrode side, Li-ions are extracted from the LiFePO$_4$ matrix and the negative reaction is represented by the Zn^{2+} ion reduction. Laboratory prototype was designed and tested (Fig 12d). Zn/LiFePO$_4$ battery offers an exceptional safe, low cost, long cycling life, and high energy and power density energy storage for large-scale applications.

4. Hollow Silica as anode material for lithium-ion batteries

Silica (silicon dioxide, SiO$_2$) attracts scientific interest as an anode for lithium-ion batteries (LIB) due to its abundance and relatively high specific theoretical capacity of 1965 mAh g^{-1}. However, during the lithiation and delithiation (alloying with Li) silica has volume expansion up to 200%, leading to its pulverisation and loss of electrical conductivity [50]. A large number of SiO$_2$ studies is aimed to improve its electrical conductivity and maintain mechanical stability [51, 52]. One of the methods is the in-situ formation of a passivating phase to increase the mechanical resistance during the volume expansion. The hollow structure of SiO$_2$ will protect it from pulverization during the lithiation and twice volume expansion, thereby prolonging battery life [53–55]. Silica was synthesized according to the published procedure [56] (Fig. 13).
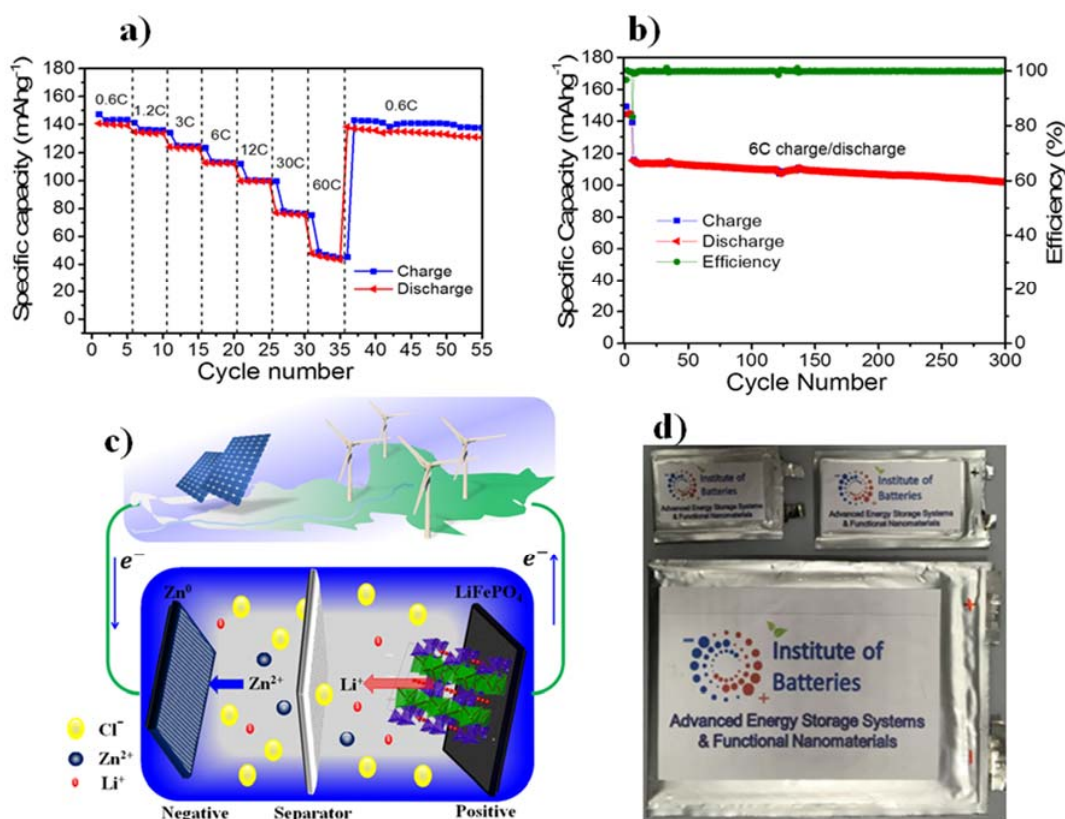

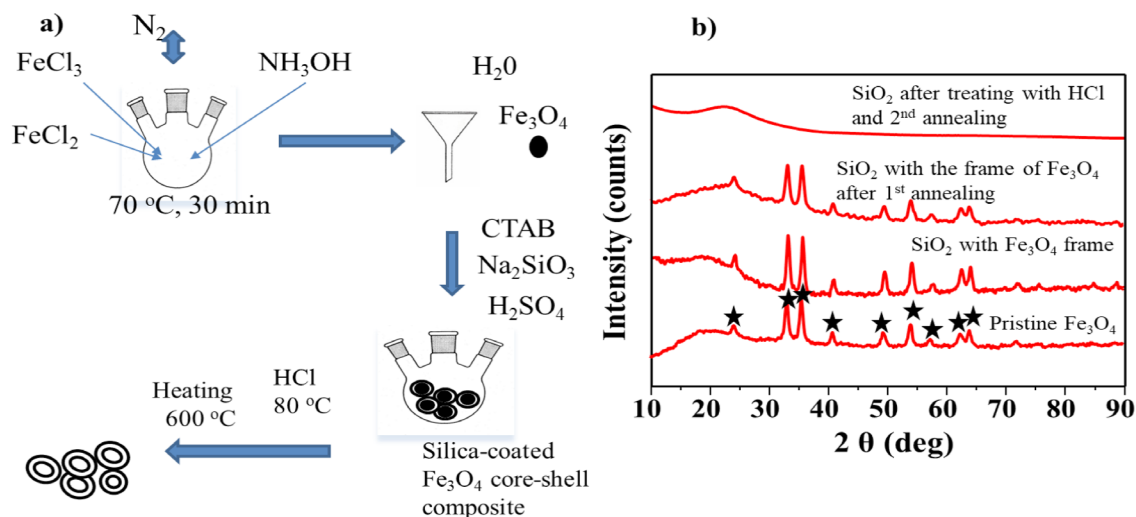Fig. 12. Electrochemical performance of Zn/LiCl-ZnCl$_2$/LiFePO$_4$ battery.

Fig. 13. Hollow SiO_2 preparation: a) scheme; b) XRD patterns of the precursors and synthesized SiO_2.

Figure 13a shows the scheme for hollow silica (SiO_2) preparation. Fe_3O_4 nanoparticles were prepared by co-precipitation method, filtered, washed by distilled water and used as the template. Cetyltrimethyl ammonium bromide (CTAB) is used as a shell structure-directing agent. Then, Na_2SiO_3 and H_2SO_4 are titrated into the Fe_3O_4 suspension. Calcination of the synthesized silica was carried out at 600 °C for 2 h in air to remove CTAB, then after dissolving of Fe_3O_4 in hydrochloric acid.

Figure 13b shows XRD patterns of changes in the precursors structure during the silica preparation. Fe_3O_4 peaks are present in the XRD curve of freshly prepared SiO_2. These peaks are also visible after the first annealing. They disappear after the treatment with hydrochloric acid and the second annealing. Finally, a single wide peak at 22-24° at 2θ angle indicates an irregular structure of amorphous SiO_2.

The structure of synthesized silica was investigated by transmission electron microscopy (TEM) (Fig. 14). A-c images were acquired at 120 keV using JEOL JEM-1400 plus microscope in TEM imaging mode, and d-f were acquired at 200 keV using JEOL ARM 200F in STEM mode.
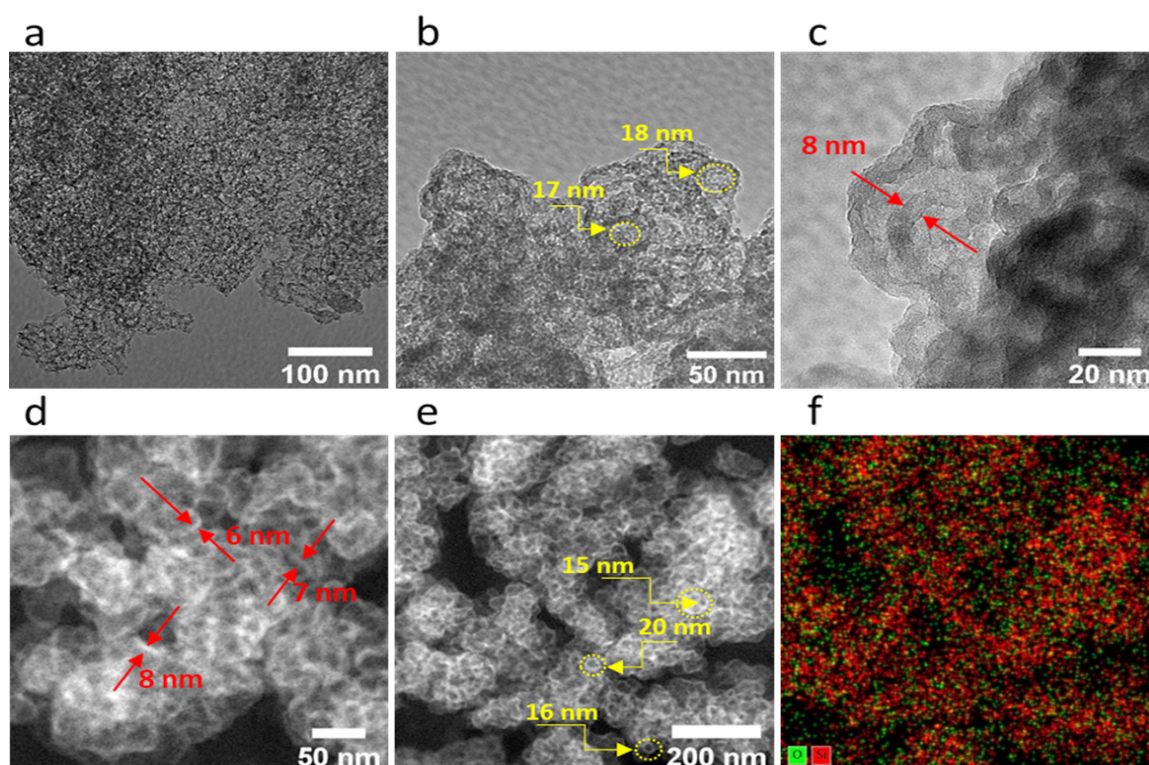
Fig. 14. Transmission electron microscopy (TEM) characterization of the SiO_2.
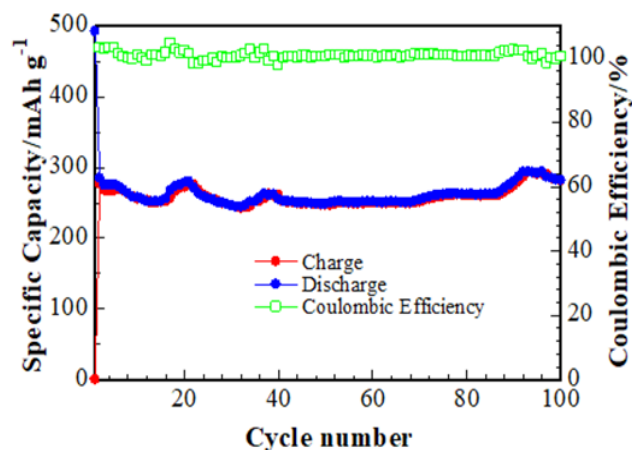
Fig. 15. Cycleability and coulombic efficiency of half-cell battery with synthesized silica.

Figure 14 (a,b,c) presents bright field TEM images of the sample at different magnifications. The SiO_2 structure has a 3D mesoporous cellular morphology. The structure is interconnected by uniformly distributed pores with 10–20 nm in window size as shown in b and e, and the wall thickness is in the range of 5–10 nm as shown in c, and d. High angle annular dark field (HAADF) scanning TEM (STEM) images of the samples at different magnification (Fig. 14 d, e). Energy-dispersive X-ray spectroscopy (EDS) elemental distribution map of Si and O element in the region in e presented in Fig. 14f. The developed 3D mesoporous SiO_2 was tested as anode material for Li|1M LiPF6 in EC:D-MC:EMC=1:1:1|SiO_2:KB:CMC coin cell and performed a stable reversible capacity of 280 mAh g^{-1} after 100 cycles at a current density 50 mA g^{-1} and excellent rate performance (Fig. 15).

This stable electrochemical performance of synthesized silica shows that using the 3D mesoporous structured SiO_2 has promising perspectives as an anode material for LIB.

5. Conclusion and perspectives

17 years past since a battery production problems in Kazakhstan were discussed [57]. Battery research was supported by Kazakhstan government well. Recent achievements of research group at Nazarbayev University on Li-ion battery were reviewed. The significant progress in areas of innovative materials for new generation batteries such as lithium-sulfur battery, three-dimensional architecture of the cell, high-capacity conversion anodes and safe aqueous battery was reported. A comprehensive consideration of all cell compo-

nents allowed to develop several prototypes of full cells. Competitive results of electrochemical performances opens the way for further scale up and investigations to satisfy the requirements of portable devices and electric vehicles.

Acknowledgment

References

[1]. Y. Zhang, Z. Bakenov, Y. Zhao, A. Konarov, T. Nam, L. Doan, K. Eun, K. Sun, A. Yermukhambetova, P. Chen, *Powder Technol.* 235 (2013) 248–255. DOI: 10.1016/j.powtec.2012.10.023

[2]. D. Liu, C. Zhang, G. Zhou, W. Lv, G. Ling, L. Zhi, Q.H. Yang, *Adv. Sci.* 5 (2018) 1700270. DOI: 10.1002/advs.201700270

[3]. Y. Zhang, Y. Zhao, A. Yermukhambetova, Z. Bakenov, P. Chen, *J. Mater. Chem. A* 2 (2013) 295–301. DOI: 10.1039/c2ta00105e

[4]. A. Yermukhambetova, Z. Bakenov, Y. Zhang, J.A. Darr, D.J.L. Brett, P.R. Shearing, *J. Electroanal. Chem.* 780 (2016) 407–415. DOI: 10.1016/j.jelechem.2015.10.032

[5]. Y. Zhang, W. Qiu, Y. Zhao, Y. Wang, Z. Bakenov, X. Wang, *Chem. Eng. J.* 375 (2019) 122055. DOI: 10.1016/j.cej.2019.122055

[6]. Y. Zhao, Z. Liu, L. Sun, Y. Zhang, Y. Feng, X. Wang, I. Kurmanbayeva, Z. Bakenov, *Beilstein J. Nanotechnol.* 9 (2018) 1677–1685. DOI: 10.3762/bjnano.9.159

[7]. W. Wang, Y. Zhao, Y. Zhang, J. Wang, G. Cui, M. Li, Z. Bakenov, X. Wang, *ACS Appl. Mater. Inter.* 12 (2020) 12763–12773. DOI: 10.1021/acsami.9b21853

[8]. J. Wang, W. Wang, Y. Zhang, Z. Bakenov, Y. Zhao, X. Wang, *Mater. Lett.* 255 (2019) 126581. DOI: 10.1016/j.matlet.2019.126581

[9]. H. Li, J. Wang, Y. Zhang, Y. Wang, A. Mentbayeva, Z. Bakenov, *J. Power Sources* 437 (2019) 226901. DOI: 10.1016/j.jpowsour.2019.226901

[10]. C. Liang, X. Zhang, Y. Zhao, T. Tan, *Nanotechnology* 29 (2018). DOI: 10.1088/1361-6528/aad543

[11]. G. Chen, J. Li, N. Liu, Y. Zhao, J. Tao, G. Kalimuldina, Z. Bakenov, Y. Zhang, *Electrochim. Acta* 326 (2019) 134968. DOI: 10.1016/j.electacta.2019.134968

[12]. Y. He, M. Li, Y. Zhang, Z. Shan, Y. Zhao, J. Li, G. Liu, C. Liang, Z. Bakenov, Q. Li, *Adv. Funct. Mater.* 30 (2020) 2000613. DOI: 10.1002/adfm.202000613

[13]. J. Liu, C. Hu, H. Li, N. Baikalov, Z. Bakenov, Y. Zhao, *J. Alloys Compd.* 871 (2021) 159576. DOI: 10.1016/j.jallcom.2021.159576

[14]. J. Zhang, W. Wang, Y. Zhang, Z. Bakenov, *ChemElectroChem* 6 (2019) 4565–4570. DOI: 10.1002/celc.201901098

[15]. A. Mentbayeva, A. Belgibayeva, N. Umirov, Y. Zhang, I. Taniguchi, I. Kurmanbayeva, Z. Bakenov, *Electrochim. Acta* 217 (2016) 242–248. DOI: 10.1016/j.electacta.2016.09.082

[16]. Y. Zhao, F. Yin, Y. Zhang, C. Zhang, A. Mentbayeva, N. Umirov, H. Xie, Z. Bakenov, *Nanoscale Res. Lett.* 10 (2015) 450. DOI: 10.1186/s11671-015-1152-4

[17]. S. Kalybekkyzy, A. Mentbayeva, M. Vezir Kahraman, Y. Zhang, Z. Bakenov, *J. Electrochem. Soc.* 166 (2019) A5396–A5402. DOI: 10.1149/2.0571903jes

[18]. Y. Zhang, Z. Bakenov, Y. Zhao, A. Konarov, Q. Wang, P. Chen, *Ionics* 20 (2014) 803–808. DOI: 10.1007/s11581-013-1042-7

[19]. S. Kalybekkyzy, A. Mentbayeva, Y. Yerkinbekova, N. Baikalov, M.V. Kahraman, Z. Bakenov, *Nanomaterials* 10 (2020) 745. DOI: 10.3390/nano10040745

[20]. W. Qiu, J. Li, Y. Zhang, G. Kalimuldina, Z. Bakenov, *Nanotechnology* 32 (2021). DOI: 10.1088/1361-6528/abc451

[21]. Y. Zhang, Y. Zhao, Z. Bakenov, D. Gosselink, P. Chen, *J. Solid State Electrochem.* 18 (2014) 1111–1116. DOI: 10.1007/s10008-013-2366-y

[22]. Y. Zhang, Y. Zhao, Z. Bakenov, *Nanoscale Res. Lett.* 9 (2014) 37. DOI: 10.1186/1556-276X-9-137

[23]. A. Mentbayeva, S. Sukhishvili, M. Naizakarayev, N. Batyrgali, Z. Seitzhan, Z. Bakenov, *Electrochim. Acta* 366 (2021) 137454. DOI: 10.1016/j.electacta.2020.137454

[24]. B. Li, Z. Sun, Y. Zhao, Z. Bakenov, *Polymers* 11 (2019) 1344. DOI: 10.3390/polym11081344

[25]. P.H.L. Notten, F. Roozeboom, R.A.H. Niessen, L. Baggetto, *Adv. Mater.* 19 (2007). DOI: 10.1002/adma.200702398

[26]. M. Nathan, D. Golodnitsky, V. Yufit, E. Strauss, T. Ripenbein, I. Shechtman, S. Menkin, E. Peled, *J. Microelectromech. Syst.* 14 (2015) 879–885. DOI: 10.1109/JMEMS.2005.851860

[27]. M. Roberts, P. Johns, J. Owen, D. Brandell, K. Edstrom, G. El Enany, C. Guery, D. Golodnitsky, M. Lacey, C. Lecoeur, H. Mazor, E. Peled, E. Perre, M.M. Shaijumon, P. Simon, P.L. Taberna, *J. Mater. Chem.* 21 (2011) 9876–9890. DOI: 10.1039/c0jm04396f

[28]. A. Nurpeissova, E. Murat, A. Adi, Z. Bakenov, *Mater. Today: Proc.* 5 (2018). DOI: 10.1016/j.matpr.2018.07.103

[29]. B. Tolegen, A. Adi, A. Aishova, Z. Bakenov, A. Nurpeissova, *Mater. Today: Proc.* 4 (2017) 4491–4495. DOI: 10.1016/j.matpr.2017.04.021

[30]. A. Nurpeissova, A. Adi, A. Aishova, A. Mukanova, S.-S. Kim, Z. Bakenov, *Int. J. Electrochem. Sci.* 13 (2018) 7111–7120. DOI: 10.20964/2018.07.75

[31]. A. Nurpeissova, A. Adi, A. Aishova, A. Mukanova, S.S. Kim, Z. Bakenov, *Mater. Today: Energy* 16 (2020) 100397. DOI: 10.1016/j.mtener.2020.100397

[32]. A. Mukanova, A. Nurpeissova, A. Urazbayev, S.S. Kim, M. Myronov, Z. Bakenov, *Electrochim. Acta* 258 (2017) 800–806. DOI: 10.1016/j.electacta.2017.11.129

[33]. G. Kalimuldina, A. Nurpeissova, A. Adylkhanova, D. Adair, I. Taniguchi, Z. Bakenov, *ACS Appl. Energy Mater.* 3 (2020) 11480–11499. DOI: 10.1021/acsaem.0c01686

[34]. A. Adylkhanova, A. Nurpeissova, D. Adair, Z. Bakenov, I. Taniguchi, G. Kalimuldina, *Front. Energy Res.* 8 (2020). DOI: 10.3389/fenrg.2020.00154

[35]. G. Kalimuldina, A. Nurpeissova, A. Adylkhanova, N. Issatayev, D. Adair, Z. Bakenov, *Materials* 14 (2021) 1615. DOI: 10.3390/ma14071615

[36]. T.S. Arthur, D.J. Bates, N. Cirigliano, D.C. Johnson, P. Malati, J. M. Mosby, E. Perre, M.T. Rawls, A.L. Prieto, B. Dunn, *MRS Bull.* 36 (2011) 523–531. DOI: 10.1557/mrs.2011.156

[37]. N. Tolganbek, A. Mentbayeva, N. Serik, N. Batyrgali, M. Naizakarayev, K. Kanamura, Z. Bakenov, *J. Power Sources* 493 (2021) 229686. DOI: 10.1016/j.jpowsour.2021.229686

[38]. H. Ragones, S. Menkin, Y. Kamir, A. Gladkikh, T. Mukra, G. Kosa, D. Golodnitsky, *Energy Fuels* 2 (2018) 1542–1549. DOI: 10.1039/c8se00122g

[39]. K. Sun, T.S. Wei, B.Y. Ahn, J.Y. Seo, S.J. Dillon, J.A. Lewis, *Adv. Mater.* 25 (2013) 4539–4543. DOI: 10.1002/adma.201301036

[40]. X. Zhu, F. Zhang, L. Zhang, L. Zhang, Y. Song, T. Jiang, S. Sayed, C. Lu, X. Wang, J. Sun, Z. Liu, *Adv. Funct. Mater.* 28 (2018). DOI: 10.1002/adfm.201705015

[41]. J. Hu, Y. Jiang, S. Cui, Y. Duan, T. Liu, H. Guo, L. Lin, Y. Lin, J. Zheng, K. Amine, F. Pan, *Adv. Energy Mater.* 6 (2016). DOI: 10.1002/aenm.201600856

[42]. N. Yesibolati, N. Umirov, A. Koishybay, M. Omarova, I. Kurmanbayeva, Y. Zhang, Y. Zhao, Z. Bakenov, *Electrochim. Acta* 152 (2015) 505–511. DOI: 10.1016/j.electacta.2014.11.168

[43]. I. Kurmanbayeva, L. Rakhymbay, K. Korzhynbayeva, A. Adi, D. Batyrbekuly, A. Mentbayeva, Z. Bakenov, *Front. Energy Res.* 8 (2020). DOI: 10.3389/fenrg.2020.599009

[44]. D. Batyrbekuly, S. Cajoly, B. Laïk, J.-P. Pereira-Ramos, N. Emery, Z. Bakenov, R. Baddour-Hadjean, *ChemSusChem* 13 (2020) 724–731. DOI: 10.1002/cssc.201903072

[45]. F. Beck, P. Rüetschi, *Electrochim. Acta* 45 (2000) 2467–2482. DOI: 10.1016/S0013-4686(00)00344-3

[46]. A. Konarov, N. Voronina, J.H. Jo, Z. Bakenov, Y.K. Sun, S.T. Myung, *ACS Energy Lett.* 3 (2018) 2620–2640. DOI: 10.1021/acsenergylett.8b01552

[47]. H. Li, L. Ma, C. Han, Z. Wang, Z. Liu, Z. Tang, C. Zhi, *Nano Energy* 62 (2019) 550–587. DOI: 10.1016/j.nanoen.2019.05.059

[48]. N. Zhang, X. Chen, M. Yu, Z. Niu, F. Cheng, J. Chen, *Chem. Soc. Rev.* 49 (2020) 4203–4219. DOI: 10.1039/c9cs00349e

[49]. C. Xu, B. Li, H. Du, F. Kang, *Angew. Chem. Int. Edit.* 51 (2012) 933–935. DOI: 10.1002/anie.201106307

[50]. L.S. Roselin, R.S. Juang, C.-Te Hsieh, S. Sagadevan, A. Umar, R. Selvin, H.H. Hegazy, *Materials* 12 (2019) 1229. DOI: 10.3390/ma12081229.

[51]. M. Yanilmaz, Y. Lu, J. Zhu, X. Zhang, *J. Power Sources* 313 (2016) 205–212. DOI: 10.1016/j.jpowsour.2016.02.089

[52]. S.D. Beattie, M.J. Loveridge, M.J. Lain, S. Ferrari, B.J. Polzin, R. Bhagat, R. Dashwood, *J. Power Sources* 302 (2016) 426–430. DOI: 10.1016/j.jpowsour.2015.10.066

[53]. X. Liu, Y. Chen, H. Liu, Z.-Q. Liu, *J. Mater. Sci. Technol.* 33 (2017) 239–245. DOI: 10.1016/j.jmst.2016.07.021

[54]. M. Ashuri, Q. He, Y. Liu, K. Zhang, S. Emani, M.S. Sawicki, J.S. Shamie, L.L. Shaw, *Electrochim. Acta* 215 (2016) 126–141. DOI: 10.1016/j.electacta.2016.08.059

[55]. N. Yan, F. Wang, H. Zhong, Y. Li, Y. Wang, L. Hu, Q. Chen, *Sci. Rep.* 3 (2013) 1568. DOI: 10.1038/srep01568

[56]. C. Liu, A. Wang, H. Yin, Y. Shen, T. Jiang, *Particuology* 10 (2012) 352–358. DOI: 10.1016/j.partic.2011.04.009

[57]. Problems of the development of battery production in Kazakhstan: materials of the round table. Almaty: Kazakh University, 2004. 84 p. (in Russian)